Numerical simulating the two-dimensional structure of the Penning discharge using the modified drift-diffusion model

S T Surzhikov

A. Ishlinsky Institute for Problems in Mechanics of the Russian academy of sciences, Vernadsky prospekt 101(1), Moscow, 119526, Russia
Dukhov All-Russian Scientific Research Institute of Automatics, Moscow, Russia

E-mail: surg@ipmnet.ru

Abstract. Spatial structure of the Penning discharge at pressures $p = 0.1 - 0.01$ Torr is investigated within the framework of the modified drift-diffusion model. This modification includes three models of elementary physical processes, which take into account peculiarities of gas discharge processes at low pressures and large reduced electric fields. Presented results of numerical simulations are in reasonable agreement with available experimental data.

1. Introduction

Electric discharges, suggested by Penning, are investigated during more than 80 years [1–3]. The basic configuration of this discharge is defined as the discharge in cylindrical chamber which is equipped by two plane cathodes and hollow anode. An axial magnetic field is a significant peculiarity of the discharge. The typical voltage drop between electrodes in such a discharge is of V~1000 V and the magnetic field induction is of ~0.1 T.

In various applications the most popular are the Penning discharge chambers at the pressures of p~10^{-2} – 10^{-5} Torr filled with the gases H_2, D_2, Ar or Xe. At such a low pressures the magnetic field plays a significant role in maintaining a gas discharge.

In spite of wide field of application of these discharges a scientific literature contains very small amount of papers containing the description of spatial structure of such discharges. Bounded number of fragmentary experimental data does not allow perform a validation of computational codes that were developed. Note that modern methods of mathematical modeling allow predict a spatial structure of gas discharges of various kind, and, unfortunately, corresponding experimental data practically absent.

Among developments of numerical simulation methods which are intended for modeling spatial structure of gas discharges, we can stay on the methods of particles in cells (PIC). Application of the method for plasma in magnetic field, including the simulation of the Penning discharge, has been demonstrated in [4-6].

However, the well known advantages of the PIC methods for simulation of rarefied plasma become helpless at increasing the pressure in discharge chambers up to order of 1 Torr. In this case the models of the magneto hydrodynamics (MHD) appear to be efficient. In turn, the MHD models lost its advantage at low pressures. It is obvious that there is a need in developing the both classes of models.

The drift-diffusion models (DDM) are the variant of the MHD models. In previous papers by the author the DDM were used for investigating the normal direct current discharge in molecular hydrogen and nitrogen in transversal magnetic field at pressure p ~ 1 Torr [7,8].

Two-dimensional model of the Penning discharge was investigated in [9-11]. Relatively high pressure of ~ 1 Torr was studied in [9,10]. This enables one to use the classical drift-diffusion model that is based on the Townsend formula. The first attempt to use the DDM for analysis of the Penning discharge at pressure p~10^{-3} Torr was made in [11], and this caused a necessity to modify the classical model. This modification concerns to two aspects.

Firstly, inside gas discharge chambers at low pressures (for example, at pressure p ~ 1 mTorr) the reduced field achieves high values of order E/p=10^6 V/cm×Torr. This means that, when calculating the mobilities it is necessary to take into account a change of physical mechanisms of interaction between charged and neutral particles under transition from low to high reduced fields [15,16].

Simple model for calculation of drift velocities of ions and electrons under transition from low to high reduced fields was proposed in [11]. The results of calculation of drift velocities using this model are shown in figure 1. It is seen that at $E/p \geq 100$ V/cm×Torr there is observable slowing down the drift velocity at increasing E/p. However, it is obvious that when E/p>10^6 V/cm×Torr this model does not work.

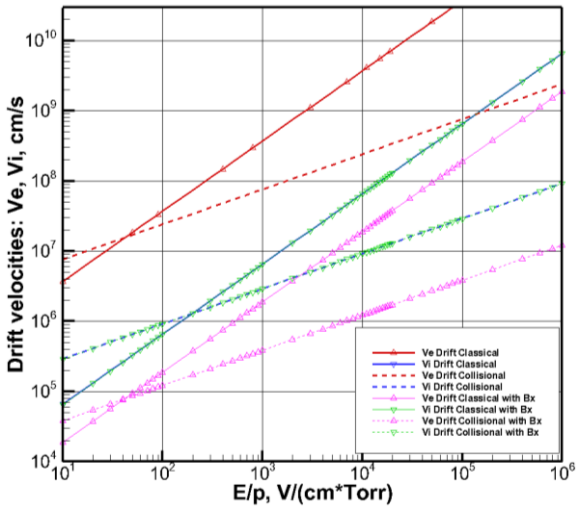

Figure 1. Drift velocities of electrons and ions versus reduce field.

The second modification relates to the method for calculation of ionizing processes at increasing E/p. It is well known that the Townsend formula gives acceptable results at E/p < 1000 V/cm×Torr (more precise, for molecular hydrogen for 150 < E/p < 600 V/cm×Torr). The model of ionization coefficient proposed in [11], is illustrated in Fig.2. It is assumed that at energy of electrons less than potential ionization of hydrogen, the Townsend formula is correct. At higher energies the ionization coefficient α is calculated as follows:

$$\alpha = N\sigma_i \ ,$$

where σ_i is the cross-section of ionizing collisions predicted by the Tompson formula:

$$\sigma_i = 4\pi a_0^2 \left(\frac{I_{H_2}}{\varepsilon} \right)^2 \cdot \frac{\left(\varepsilon - I_{H_2} \right)}{I_{H_2}} \ , \text{cm}^2.$$

Here, I_{H_2} is the potential of ionization of H_2, $4\pi a_0^2 = 3.52\times10^{-16}$ cm^2; a_0^2 is the Bohr radius, and ε is the energy of electrons (as a rule, I_{H_2} and ε are measured in eV).

For cross-linking of numerical values of the first ionization coefficient final formula is wondered as:

$$\alpha = pA^* \exp\left[-B/(E/p)\right],$$

where A^*=2.75 1/cm×Torr; B = 130 V/cm×Torr.

According to figure 2 the ionization coefficients firstly increase and then decrease as E/p decreases.

So, in the Penning discharge used as the ions accelerator, there are two competitive mechanisms at applied voltage drop increasing, namely, a decreasing of ionization efficiency, and an increasing of charged particle energies.

In the present work the modified DDM is applied for analysis the Penning discharge at the pressure p = 0.01÷0.1 Torr. At these pressures the classical DDM cannot be applied for modeling the gas discharge chamber with size of ~ 1cm. Under these conditions typical reduced fields do not exceed the values of $E/p \sim 10^4$ V/cm×Torr.

Note, that reduced field in gas discharge chamber depends not only on applied voltage drop, but also on the configuration of volume charge.

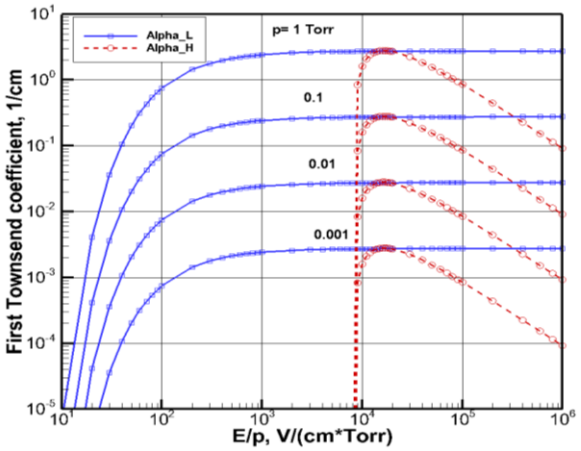

Figure 2. Ionization coefficient for modified DDM at pressure p=1.0÷0.001 Torr.

2. Governing equations

A cylindrical two-dimensional 2D glow discharge in molecular hydrogen between flat electrodes with a presence of axial magnetic field is considered (see figure.3).

A modified drift-diffusion model [10] (MDDM) is used for description of gas discharge processes. This theory is based on the continuity equations for electron and positive ion concentrations n_e and n_i together with the equations for the electro-static field $\mathbf{E} = -\text{grad}\varphi$. The governing equations of the drift-diffusion theory with axial magnetic field have the following form:

$$\frac{\partial n_e}{\partial t} + \frac{\partial \Gamma_{e,x}}{\partial x} + \frac{1}{r}\frac{\partial r\Gamma_{e,y}}{\partial r} = \dot{\omega}_i = \alpha(E)\left|\mathbf{\Gamma}_e\right| - \beta n_i n_e \ , \qquad (1)$$

$$\frac{\partial n_i}{\partial t} + \frac{\partial \Gamma_{i,x}}{\partial x} + \frac{1}{r}\frac{\partial r\Gamma_{i,y}}{\partial r} = \dot{\omega}_i = \alpha(E)\left|\mathbf{\Gamma}_e\right| - \beta n_i n_e \ , \qquad (2)$$

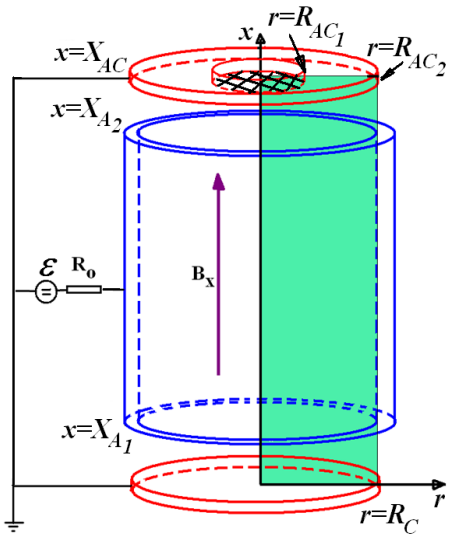

Figure 3. Schematic representation of a glow discharge in external magnetic field.

$$\frac{\partial^2\varphi}{\partial x^2}+\frac{1}{r}\frac{\partial}{\partial r}r\frac{\partial\varphi}{\partial r}=4\pi e(n_e-n_i)\ , \tag{3}$$

where

$$\mathbf{\Gamma}_e=n_e\mathbf{u}_e=-\hat{\mathbf{D}}_e\mathrm{grad}n_e-n_e\hat{\boldsymbol{\mu}}_e\mathbf{E}\ ,\ \mathbf{\Gamma}_i=n_i\mathbf{u}_i=-\hat{\mathbf{D}}_i\mathrm{grad}n_i+n_i\hat{\boldsymbol{\mu}}_i\mathbf{E}\ ,$$

$$\hat{\mathbf{D}}_e=\begin{pmatrix}D_{e,x}&0\\0&\dfrac{D_{e,r}}{1+b_e^2}\end{pmatrix},\ \hat{\mathbf{D}}_i=\begin{pmatrix}D_{i,x}&0\\0&\dfrac{D_{i,r}}{1+b_i^2}\end{pmatrix},\ \hat{\boldsymbol{\mu}}_e=\begin{pmatrix}\mu_{e,x}&0\\0&\dfrac{\mu_{e,r}}{1+b_e^2}\end{pmatrix},\ \hat{\boldsymbol{\mu}}_i=\begin{pmatrix}\mu_{i,x}&0\\0&\dfrac{\mu_{i,r}}{1+b_e^2}\end{pmatrix}, \tag{4}$$

$$\mathbf{j}=e(\mathbf{\Gamma}_i-\mathbf{\Gamma}_e),$$

$\alpha(E)$ and β are the ionization and recombination coefficients, $\mathbf{\Gamma}_e$ and $\mathbf{\Gamma}_i$ are the electron and ion flux densities, μ_e and μ_i are the electron and ion mobility, D_e and D_i are the electron and ion diffusion coefficients, φ is the potential of electric field, $\mathbf{u}_e$ and $\mathbf{u}_i$ are the averaged velocities of electrons and ions, $\mu_e=\dfrac{e}{m_e\nu_e}$ and $\mu_i=\dfrac{e}{m_i\nu_{in}}$ are the electrons and ions mobilities, $D_e=\dfrac{kT_e}{e}\mu_e$ and $D_i=\dfrac{kT_i}{e}\mu_i$ are the electrons and ions diffusion coefficients, ν_{en},ν_{ei} and ν_{in} are the frequencies of electron-neutral, electron-ion, and ion-neutral collisions, $\nu_e=\nu_{en}+\nu_{ei}$, T_e and T_i are the temperatures of electrons and ions.

Taking into account that the magnetic field has only x-component B_x (see figure 3), one can write:

$$\Gamma_{e,x}=n_eu_{e,x}=\left(-D_e\frac{\partial n_e}{\partial x}-\mu_en_eE_x\right),\quad \Gamma_{e,r}=n_eu_{e,r}=\frac{1}{1+b_e^2}\left(-D_e\frac{\partial n_e}{\partial r}-\mu_en_eE_r\right),$$

$$\Gamma_{e,\varphi}=n_eu_{e,\varphi}=-b_e\Gamma_{e,r},$$

$$\Gamma_{i,x}=n_iu_{i,x}=\left(-D_i\frac{\partial n_i}{\partial x}-\mu_in_iE_x\right),\quad \Gamma_{i,r}=n_iu_{i,r}=\frac{1}{1+b_i^2}\left(-D_i\frac{\partial n_i}{\partial r}+\mu_in_iE_r\right),$$

where $b_e=\dfrac{\mu_e}{c}B_x$ and $b_i=\dfrac{\mu_i}{c}B_x$ are the Hall parameters of electrons and ions.

The source term in the right hand side can be written as following

$$\left|\mathbf{\Gamma}_e\right| = \sqrt{\Gamma_{e,x}^2 + \Gamma_{e,r}^2 + \Gamma_{e,\varphi}^2} \ . \tag{5}$$

Note that the azimuthal component of electronic flux $\Gamma_{e,\varphi}$ can be significant due to the condition $b_e >> 1$.

The introduced coefficients, which are taking into account a physically meaningful magnetic field, can be presented in the following form:

$$b_e = \frac{\mu_e B_x}{c} = \frac{\omega_e}{\nu_e}, \qquad b_i = \frac{\mu_i B_x}{c} = \frac{\omega_i}{\nu_{in}},$$

where

$\omega_e = \frac{eB_x}{m_e c}$ and $\omega_i = \frac{eB_x}{m_i c}$ are the Larmor frequencies of electrons and ions, m_e and m_i are the masses of electrons and ions.

The boundary conditions for charged particles and electrical potential are formulated as following:

$$x = X,\ r < R_{AC_1}: \qquad \frac{\partial n_i}{\partial x} = 0, \Gamma_e = \gamma^* \Gamma_i,\ \varphi = 0,$$

$$x = 0; x = X,\ r > R_{AC_1}: \ \frac{\partial n_i}{\partial x} = 0, \Gamma_e = \gamma \Gamma_i,\ \varphi = 0, \tag{6}$$

where γ is the coefficient of the secondly ion-electron emission, γ* is the effective coefficient of the secondly ion-electronic emission, which is taken of the order $\gamma^* \sim (10^{-1} - 10^{-2})\gamma$.

For cylindrical surface of anode the following boundary conditions were used:

$$X_{A_1} < x < X_{A_2},\ r = R_C: \ \frac{\partial n_e}{\partial r} = 0,\ n_i = 0,\ \varphi = V \ .$$

For cylindrical surface between anode and cathode:

$$X_{A_1} > x,\ r = R_C: \ \frac{\partial n_e}{\partial r} = \frac{\partial n_i}{\partial r} = \frac{\partial \varphi}{\partial r} = 0 \ ,$$

$$X_{A_2} < x,\ r = R_C: \ \frac{\partial n_e}{\partial r} = \frac{\partial n_i}{\partial r} = \frac{\partial \varphi}{\partial r} = 0 \ . \tag{7}$$

A quasi-neutral plasma cloud of a spherical shape in the center of the chamber is used as the initial condition.

The transport and thermo-physics properties do not depend on temperature (for H_2), therefore:

$$\mu_e(p) = \frac{3.7 \cdot 10^5}{p}, \frac{\mathrm{cm}^2}{\mathrm{V \cdot s}}, \ \mu_i(p) = \frac{6.55 \cdot 10^3}{p}, \frac{\mathrm{cm}^2}{\mathrm{V \cdot s}},$$

$$D_e = \mu_e(p) T_e, \qquad D_i = \mu_i(p) T_i,$$

where p is the pressure in Torr.

The recombination coefficient β and electron temperature are taken as constants $\beta = 2 \times 10^{-7}$ cm^3/s and $T_e = 11610\mathrm{K}$.

The ionization coefficient for H_2 is determined as follows (the 1st Townsend formula):

$$\alpha(E) = p^* A^* \exp\left[-\frac{B}{\left(|\mathbf{E}|/p^*\right)} \right], \text{cm}^{-1},$$

where $A^* = 2.75 \frac{1}{\text{cm} \cdot \text{Torr}}$, $B = 130 \frac{\text{V}}{\text{cm} \cdot \text{Torr}}$.

Equations (1)–(3) are supplemented with the equation for the external electric circuit (see figure 1), which is written for a stationary current as

$$\mathcal{E} = V + IR_0 \ ,$$

where V is the voltage on the electrodes, I is the total discharge current, $\mathcal{E}$ is the e.m.f. in power supply, and R_0 is the external resistance.

The modified drift-diffusion model includes two modifications of the classical DDM, namely, the modification of drift mobilities and the modification of velocity of ionization.

In Ref.[10] it was suggested to use the following relations for ion and electron mobilities

$$\mu_{i,eff} = \min\left\{ \frac{\mu_i p}{p}, \frac{9.2 \cdot 10^4}{\sqrt{p_{Torr} E_V}} \right\}, \quad \mu_{e,eff} = \min\left\{ \frac{\mu_e p}{p}, \frac{2.4 \cdot 10^6}{\sqrt{p_{Torr} E_V}} \right\}, \tag{8}$$

and for corresponding diffusion coefficients

$$D_{i,eff} = \mu_{i,eff} T_i, \ D_{e,eff} = \mu_{e,eff} T_e .$$

This gives a possibility to use classical definitions for drift velocities

$$\boldsymbol{V}_{dr,i} = \mu_{i,eff} \mathbf{E}, \ \boldsymbol{V}_{dr,e} = \mu_{e,eff} \mathbf{E}.$$

The ionization coefficient for H_2 is determined as follows:

$$\alpha_{low}(E) = pA^* \exp\left[-\frac{B}{\left(|\mathbf{E}|/p\right)} \right], \ \text{cm}^{-1}, \ \text{at low reduced fields} \tag{9}$$

and

$$\alpha_{high} = N_n \sigma_i \ \ , \text{cm}^{-1}, \text{ for high reduced fields,} \tag{10}$$

where the ionization cross section σ_i could be calculated using the Tomson formula

$$\sigma_i = 4\pi a_0^2 \left(\frac{I_{H_2}}{\varepsilon} \right)^2 \cdot \frac{\left(\varepsilon - I_{H_2}\right)}{I_{H_2}} \ , \text{cm}^2.$$

Instead of the reduced fields we can use the dependence on the electron and ion energies, where kinetic energies are estimated as following:

$$\varepsilon_{[eV]} = 2.84 \cdot 10^{-14} V^2_{e[cm/s]}, \quad \varepsilon_{[eV]} = 1.05 \cdot 10^{-12} V^2_{i[cm/s]} .$$

Now in the MDD model we can formulate constitutive relations for electrons:

$$\Gamma_{e,x} = -D_{e,eff} \frac{\partial n_e}{\partial x} - \mu_{e,eff} n_e E_x \ ,$$

$$\Gamma_{e,r} = -\frac{D_{e,eff}}{1 + b^2_{e,eff}} \frac{\partial n_e}{\partial r} - \frac{\mu_{e,eff}}{1 + b^2_{e,eff}} n_e E_r \ ,$$

$$\Gamma_{e,\varphi} = -b_{e,eff}\Gamma_{e,r}, \quad b_{e,eff} = \frac{\mu_{e,eff}B_x}{c},$$

and for ions:

$$\Gamma_{i,x} = -D_{i,eff}\frac{\partial n_i}{\partial x} + \mu_{i,eff} n_i E_x,$$

$$\Gamma_{i,r} = -\frac{D_{i,eff}}{1+b_{i,eff}^2}\frac{\partial n_i}{\partial r} + \frac{\mu_{e,eff}}{1+b_{i,eff}^2} n_i E_r,$$

$$\Gamma_{i,\varphi} = -b_{i,eff}\Gamma_{i,r}, \quad b_{i,eff} = \frac{\mu_{i,eff}B_x}{c}.$$

3. Results of numerical simulation

The calculations were performed for the following initial data: the pressure in molecular hydrogen H_2 was of p=0.1 ÷ 0.01 Torr; e.m.f. of power supply E =200 V, R_0 = 3000 Ohm, $\gamma = 0.33$, $\gamma^* \sim 10^{-2}\gamma$, $B_x = 0.1$T, $R_C = R_{AC_2} = 0.55$ cm, $R_{AC_1} = 0.2$ cm, $X_{A_1} = 0.425$ cm, $X_{A_2} = 0.675$ cm, and X_C =1.1 cm (this value was used as a spatial scale of the problem under consideration).

Figure 4 shows the electron and ion concentrations in discharge chamber at pressures p=0.1 and 0.01 Torr. The main feature of these distributions is high concentrations of charged particles in the central domain of the discharge chamber at high pressure and low concentrations when the pressure is low.

Distributions of electron and ion concentrations at pressures p=0.1 Torr (left picture) and p=0.01 Torr (right picture) are shown in figure 4. At low pressure the domain of volume charge is shifted to internal cylindrical surface of the anode.

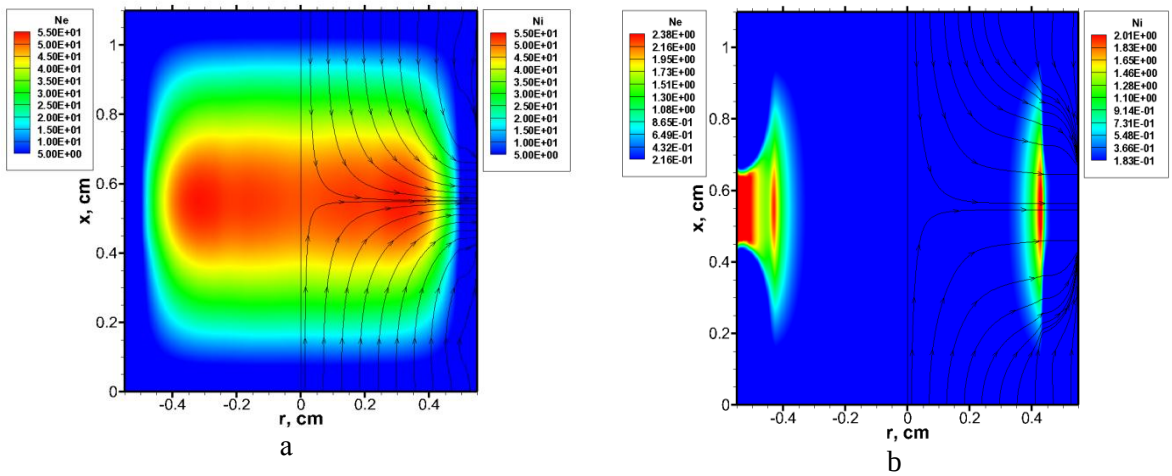

Figure 4. Concentration of (a) electrons Ne and (b) ions Ni (in 10^{10} cm^{-3}).

Decreasing of the pressure leads to significant change of the reduced field in the gas discharge chamber. From figure 5 one can see that near anode the reduced field E/p sharply increases, whereas in the volume the reduced field is distributed quite smoothly. The distribution of the ionization coefficient (see figure 6) corresponds to this distribution of the reduced field.

Differences between coefficients of ionization α_x and α_r, corresponding to the axial and radial fluxes of electrons points out to a "switching" from one dependence to another (see relations (9), (10)).

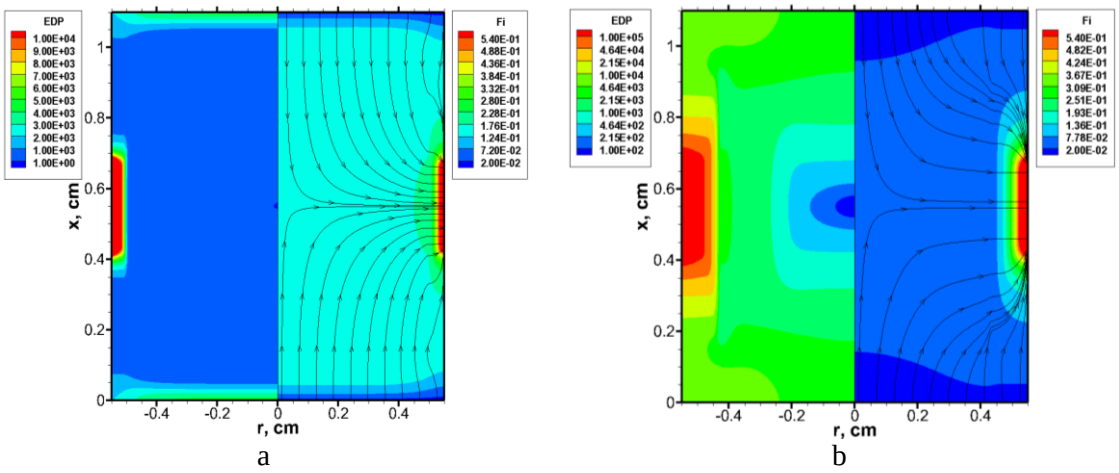

Figure 5. (a) Reduced field (EDP=E/p in V/(cm*Torr)) and (b) electric potential (Fi = $\varphi/\mathcal{E}$) at $p = 0.1$ Torr and $p = 0.01$ Torr.

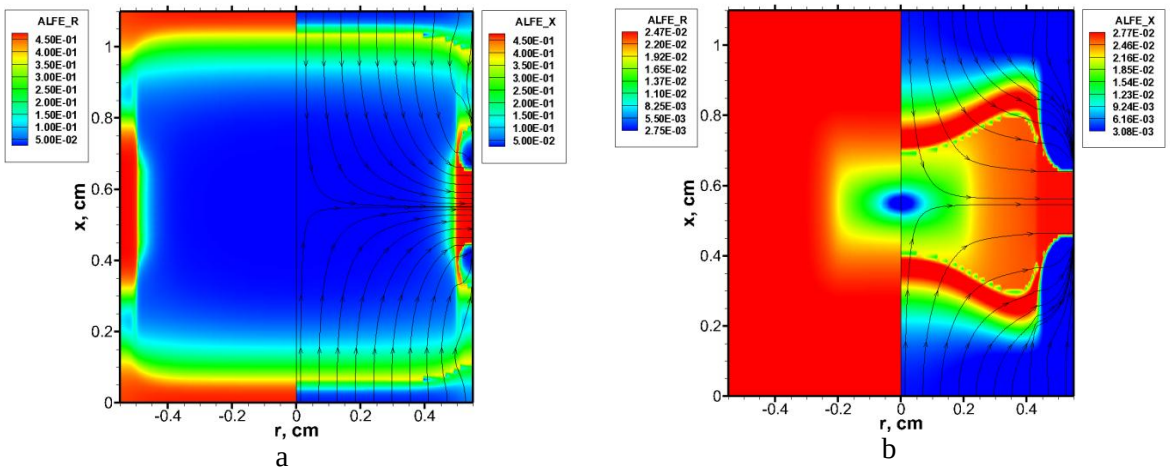

Figure. 6. Coefficients of ionization (in 1/cm) at (a) $p = 0.1$ Torr and (b) at $p = 0.01$ Torr; ALFE_R=α_r is the coefficient of ionization calculated with E_r, ALFE_X=α_x is the coefficient of ionization calculated with E_x.

It is seen that at $p = 0.1$ Torr these differences are insignificant, whereas at $p = 0.01$ Torr the efficiency of ionization of neutral particles induced by electron collisions are different.

The source term $\dot{\omega}_i$ in Eqs.(1) and (2) is shown for two pressures in figure 7. This term is decreased by two order of the value when the pressure is decreased one order of the value. The volume of increased ionization is located near anode. So, such model of ionization in the Penning discharge gives low efficiency of ionization in the discharge volume. Nevertheless, presented results of numerical simulations are in reasonable qualitative agreement with available experimental data [1-3].

Axial distributions of ion and electron velocities in the Penning discharge at pressures $p = 0.1$ Torr and $p = 0.01$ Torr are shown in figure 8. The corresponding axial distributions of the reduced electric field and the energy of electrons, which were calculated using the axial velocity of electrons, are shown in figure 9.

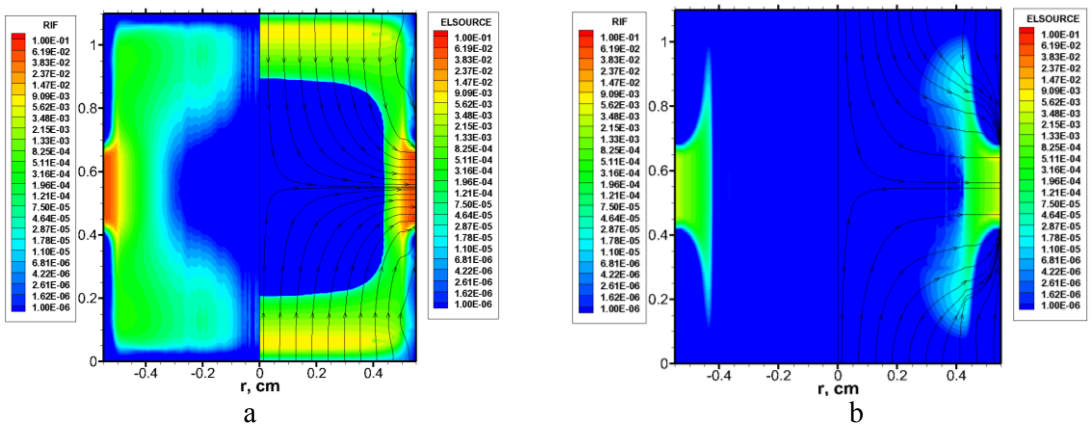

Figure. 7. Source of ionization ELSOURCE= $\dot{\omega}_i$ (in 10^{20}/(cm^3*s)) at (a) p=0.1 Torr and (b) p=0.01 Torr. Left parts of the figures show source of ionization due to azimuthal movement of electrons.

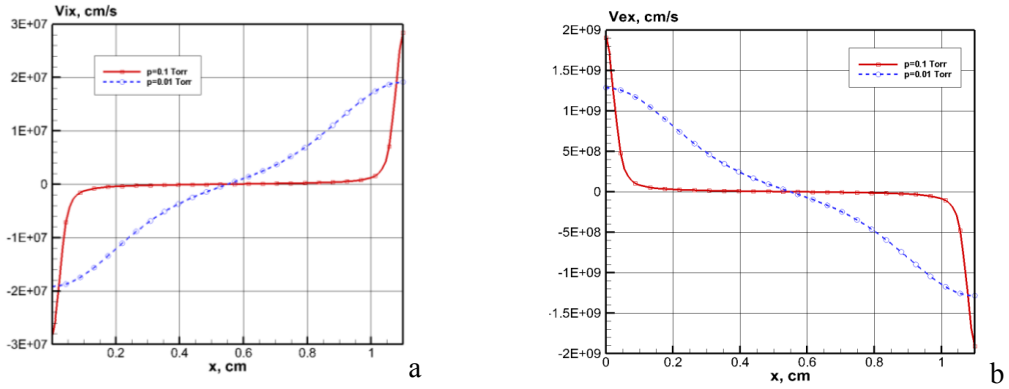

Figure. 8. Axial distributions of (a) ion and (b) electron average velocities in x-direction at the pressure p=0.1 Torr and 0.01 Torr.

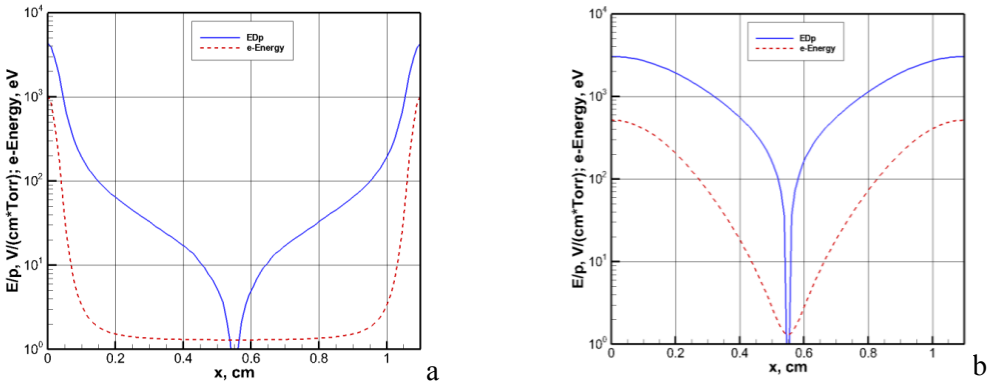

Figure 9. Axial distribution of reduced field (in V/(cm*Torr) and electron energy in eV at the pressure p=0.1 Torr and 0.01 Torr.

Conclusion

Spatial structure of the Penning discharge at pressures p = 0.1 – 0.01 Torr has been investigated within the framework of the modified drift-diffusion model. This modification includes three models of elementary physical processes, which take into account peculiarities of gas discharge processes at low pressures and large reduced electric fields. These are:

1) The non-linear model of behavior of ion and electron drifts depending on the reduced electric field in wide range of variation ;
2) The model of ionization of neutral particles in collisions with electrons in wide range of variation of the reduced electric field;
3) The anisotropic model of ionization by the axial, radial, and azimuthal fluxes of electrons.

The analysis of the presented predictions of spatial structure of the Penning discharge using the modified drift-diffusion model allows to suggest that the significant disadvantage of the model consists in an absent of the explicit source term connected with the low-energy electrons that were born in gas discharge volume after the first acts of ionizations by the high-energy electrons, being accelerated near cathode and anti-cathode. Presented MDD model should be improved in this aspect.

Acknowledgments
The work was supported by the Russian Science Foundation grant # 16-11-10275.

References
[1] Penning F M 1936 The Glow Discharge at Low Pressure Between Coaxial Cylinders in an Axial Magnetic Field *Fhysica III* (9) pp 873-894
[2] Hirsch E N 1964 On the Mechanizm of The Penning Discharge *Brit. J. Appl. Phys.* **15** pp 1535-1544
[3] Safronov B G , Konovalov V G 1974 Investigation of a Penning Discharge at Low Pressure. *NASA Technical Translation NASA TT F-15,523* p 14
[4] Birdsall C K , Langdon A B 1985 Plasma Physics, via Computer Simulation. *McGraw-Hill, New York* p 464
[5] Surzhikov S T 1999 Expansion of Multi-Charged Plasma Clouds Into Ionospheric Plasma With Magnetic Field. *Journal of Spacecraft and Rockets* **36**(6) pp 907-911
[6] Dikalyuk A S 2017 Development of Particle-in-Cell Solver for Numerical Simulation of Penning Discharge *AIAA 2017-0842* p 22
[7] Surzhikov S T, Shang J S 2014 Normal Glow Discharge in Axial Magnetic Field *Plasma Sources Sciences and Technology* **23**(054017) p 8
[8] Surzhikov S T 2016 Drift-Diffusion Model of Normal Glow Discharge in an Axial Magnetic Field *Doklady Physics* **61**(12) pp 596-600
[9] Surzhikov S T 2017 The Two-Dimensional Structure of the Penning Discharge in a Cylindrical Chamber with Axial Magnetic Field at Pressure of about 1 Torr *Technical Physics Letters* **43**(2) pp 169-172
[10] Surzhikov ST 2017 Numerical Study of Acceleration of the Hydrogen Ions in the Penning Discharge at Pressures Around 1 Torr *AIAA 2017-0155* p 13
[11] Surzhikov S T 2015 Application of the Modified Drift-Diffusion Theory to Study of the Two-Dimensional Structure of the Penning Discharge *AIAA 2015-1832* p 27
[12] Von Engel A, and Steenbeck M 1932 Elektrische Gasentladungen, Vol.II *Springer, Berlin* p 68
[13] Surzhikov S T 2013 Computational Physics of Electric Discharges in Gas Flows *Walter de Gruyter, Berlin/Boston* p 428
[14] Shang J S 2016 Computational Electromagnetic-Aerodynamics *Wiley, Hoboken, New Jersey* p 424
[15] Huxley L G H , Crompton R W 1974 The Diffusion and Drift of Electrons in Gases *John Wiley & Sons. New York* p 669
[16] McDaniel E W 1964 Collision Phenomena in Ionized Gases *John Wiley & Sons, Inc., New York* p 797 p
[17] McDaniel E W, Mason E A 1973 The Mobility and Diffusion of Ions in Gases *Willey and Sons, New York, London, Sydney, Toronto* p 381